Penerbit Akademia Baru

CFD Letters

Journal homepage: www.akademiabaru.com/cfdl.html
ISSN: 2180-1363

Effect of Nanofluids on Heat Transfer and Pressure Drop Characteristics of Diverging-Converging Minichannel heat sink

Open Access

Nura Mu'az Muhammad[1,2,*], Nor Azwadi Che Sidik[1], Aminuddin Saat[1], Bala Abdullahi[2]

[1] Faculty of Mechanical Engineering, Universiti Teknologi Malaysia, 81310 Skudai, Johor, Malaysia
[2] Faculty of Engineering, Kano University of Science and Technology, Wudil, Nigeria

ARTICLE INFO

Article history:
Received 3 January 2019
Received in revised form 16 April 2019
Accepted 22 April 2019
Available online 26 April 2019

Keywords:
Nanofluid, Heat enhancement, thermal devices, Nusselt number, divergent-convergent,

ABSTRACT

Combine effects of nanofluid and variable cross-section minichannel heat sink has become a remarkable option for efficient cooling of thermal devices like miniature electronic devices and compact heat exchangers. In this paper, the single-phase numerical method was employed to study the effect of different nanofluids on heat transfer and pressure drop penalty in the Diverging-converging minichannel heat sink (DCMCHS). CFD analysis carried out using commercial ANSYS software employing the finite volume method. The nanofluids are prepared as stable nanoparticles of Al_2O_3, Cu, and SiO_2 and suspended in deionized water with concentrations of 0-0.8% volume. The DCMCHS subjected to a uniform heat flux of 45000 W/m^2 and the fluid flow within the transition's region with Reynolds number 2000 to 2300. The validations of numerical data conducted with results from empirical correlations exhibit a good agreement with about 9% deviation. The results revealed an insignificant change in pressure drops with a variation of nanofluids loadings, whereas, the increase in Reynolds number and nanoparticle loading indicated a considerable influence on the enhancement of heat transfer coefficient. Al_2O_3–water nanofluid shows better performance in terms of heat transfer than other nanofluids. The results indicate that nanofluid and DCMC can enhance the hydro-thermal performance of the heat sink.

Copyright © 2019 PENERBIT AKADEMIA BARU - All rights reserved

1. Introduction

Thermal management of heat sinks and heat exchangers have become a dynamic process due to ever-changing needs by the users and manufacturing constraints in the devices. Electronic devices like IC and heat exchangers are decreasing in size with the expectation to offer high performance with better efficiency and use less energy. These requirements make their thermal performance a difficult task. Air and conventional thermal liquids failed to provide the desired heat dissipation effect due to their low thermal conductivity. Researches were undertaking to unravel the challenges posed by thermal management in electronic and process industries either experimentally or numerically using either a single phase or multiphase by developing models to predict the results [1-6].

* *Corresponding author.*
E-mail address: nuramuaz@gmail.com (Nura Mu'az Muhammad)

Nanofluid has shown the remarkable performance as heat transfer fluid due to its enhanced thermophysical properties than the base fluid. Since the initial work of Choi [7] on new thermal fluid coined "nanofluid," many pieces of research were conducted to exploit the benefits of using nanofluid as thermal fluid for heat transfer enhancement of the thermal system. They gave much consideration to factors that affect its thermal conductivity and viscosity, such as nanoparticles material, size and shape, concentration, properties of the base fluid and sometimes additional substances like surfactant and Ph value. [8, 9]. This innovative thermal fluid characterized by nano-sized particles usually in the order of 1 -100 nm synthesized using stable techniques and dispersed through either single step or two steps methods to form a nanofluid with excellent thermal properties. Many researchers employed these varieties of nanoparticles such as metals [10], metal oxides [11], carbides [12] and carbon-based such as Carbon nanotubes (CNT) and graphene [13-15].

Presently, use of nanofluids in micro and minichannels are intensively studied and well-reviewed [16-18], yet there is inconsistency in the results obtained from the studies conducted on nanofluids in minichannels, while some researchers observed some emerging phenomena. There is an increase in recognition of the use of combined passive techniques of nanofluid and minichannel for high heat flux removal in thermal system management. Performance evaluation of minichannel solar collector was conducted by Mahian *et al.,* [19] with four dissimilar water-based nanofluids of nanoparticle size of 25 nm comprising Cu, Al_2O_3, TiO_2, and SiO_2 at concentration up to 4% and found that Al_2O_3-H_2O and SiO_2-H_2O nanofluids revealed the highest and lowest heat transfer coefficient, respectively. Sohel *et al.,* [20] used a circular shaped copper minichannel heat sink having hydraulic diameter of 500 µm to study performances of various aqueous nanofluids including Al_2O_3-H_2O, Cu-H_2O, and Ag-H_2O, they observed that heat transfer rate significantly increase by the increase of volume fraction of nanoparticle, and Ag-Water nanofluid has the highest performance possibly due to the high thermal conductivity of its particle. Transient heat transfer and flow analysis in a multi-pass crossflow minichannel heat exchanger using mixture of Alumina-water-Ethylene glycol considered as homogenous single-phase fluid was carried out by Ismail *et al.,* [21] and revealed that nanofluid has better convective heat transfer in contrast to the base fluid and at 3vol.% it reaches quasi-steady condition earlier than that of base fluid.

Researchers observed that the reduction of hydraulic diameter and higher heat transfer surface area per unit fluid volume of nanoparticles could effectively remove excess heat and improves the heat transfer coefficient (HTC). Thus, they introduced a lot of methods like changing minichannel geometrical parameters, such as channel number, aspect ratio, cross-sections and path configurations [22]. Khoshvaght *et al.,* [23] studied the use of Al_2O_3–H_2O nanofluid in the twisted minichannel (TMC) having various structural parameters for laminar flow and heat transfer characteristics using a 3D numerical scheme for Re within 300 to 1500. The results indicated that all the TMCs tested, possessed improved heat transfer than the smooth circular minichannel and found that Heat transfer coefficient and pressure drop are higher for nanofluid compared to a base fluid for all the cases.

Ajeel *et al.,* [24] used a symmetrically semicircle-corrugated channel with SiO_2-water nanofluid to investigate the geometrical effect of height and pitch of corrugation on the hydrothermal behaviors of forced convective heat transfer and flow under Reynolds number and nanoparticles concentration of 10000- 30000 and 0-8% vol., respectively. The results showed enhancement of average Nusselt number as Reynolds number appreciated and with the corrugated channel height, and the optimum parameters for substantial heat transfer enhancement were found in corrugation height and pitch of 2.5 mm and 15 mm respectively. Hassan *et al.,* [25] numerically investigated the effect on the heat transfer and fluid flow improvement using unique types of nanofluids to cool a Central Processing

Unit (CPU) system. They found that SiO_2 has the highest coefficient of skin friction, and followed in descending magnitude by Al_2O_3, ZnO, and CuO.

From the prior research works, the effect of different nanofluids in diverging-converging minichannel for heat transfer and flow analysis as combined passive heat transfer enhancement techniques are rarely investigated, and previous studies have not treated it with due diligence. Thus, the authors of this work believe that the study using the minichannel geometry combined with various nanofluids can offer more insight into the thermal management of electronic devices. The primary objective of the current work is to demonstrate the performance of the diverging-converging minichannel in terms of heat transfer and flow characteristics by studying the effect of nanofluid types, concentrations, and physical-thermal properties, and the consequences on pressure drop.

2. Methodology

This section presented a description of physical models, computational domain adopted, working thermal fluids used, assumptions, mathematical governing equations, and imposed boundary conditions about the geometry and model.

2.1 Model Geometry

The physical model considered in the numerical analysis of the divergent-convergent minichannel heat sink (DCMCHS) was used in the previous work by the authors [26] and shown in Figure 1 (a). It is made up of aluminium material and has ten parallel channels each of width and height of 1mm and 1.25mm, respectively. The nanofluid flow through the channels of the DCMCHS placed on an electronic chip and removed heat by convection from a heat dissipated by the chip. A single channel as illustrated in Figure 1(b) was modeled and used to reduce the size of grid elements and save computational time.

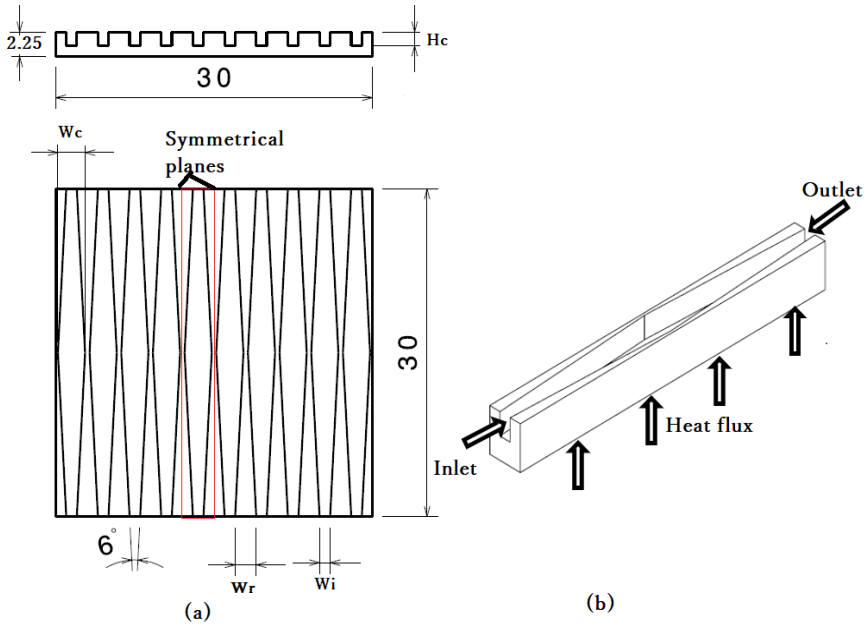

Fig. 1. (a) 3D Illustration of DCMCHS and (b) Single channel Computational domain

2.2 Governing Equations

Nanofluids are produced from fine particles in nanometre scale dispersed in water, and the nanoparticles and base fluid are assumed to flow with equal velocity, and there exist thermal equilibrium between them. Also, the nanofluid flow is assumed laminar, incompressible and Newtonian. We considered the problem as a steady-state and the conservation equations for continuity, momentum, and energy in the fluid are respectively given as:

The mass conservation equation:

$$\frac{\partial u}{\partial x}+\frac{\partial v}{\partial y}+\frac{\partial w}{\partial z}=0 \tag{1}$$

while momentum equations in x, y, and z cartesian coordinates, respectively given as:

$$u\frac{\partial u}{\partial x}+v\frac{\partial u}{\partial y}+w\frac{\partial u}{\partial z}=-\frac{1}{\rho}\frac{\partial P}{\partial x}+\frac{\mu}{\rho}\left(\frac{\partial^2 u}{\partial x^2}+\frac{\partial^2 u}{\partial y^2}+\frac{\partial^2 u}{\partial z^2}\right) \tag{2}$$

$$u\frac{\partial v}{\partial x}+v\frac{\partial v}{\partial y}+w\frac{\partial v}{\partial z}=-\frac{1}{\rho}\frac{\partial P}{\partial y}+\frac{\mu}{\rho}\left(\frac{\partial^2 v}{\partial x^2}+\frac{\partial^2 v}{\partial y^2}+\frac{\partial^2 v}{\partial z^2}\right) \tag{3}$$

$$u\frac{\partial w}{\partial x}+v\frac{\partial w}{\partial y}+w\frac{\partial w}{\partial z}=-\frac{1}{\rho}\frac{\partial P}{\partial z}+\frac{\mu}{\rho}\left(\frac{\partial^2 w}{\partial x^2}+\frac{\partial^2 w}{\partial y^2}+\frac{\partial^2 w}{\partial z^2}\right) \tag{4}$$

Where u, v and w represent the velocity components in x, y and z directions, respectively. Also, P, ρ and μ represent the pressure drop, mass density and dynamic viscosity of the fluid, respectively. The energy equations for the fluid and solid domains are respectively given in Eq. (5) and Eq. (6) as:

$$u\frac{\partial T_f}{\partial x}+v\frac{\partial T_f}{\partial y}+w\frac{\partial T_f}{\partial z}=\frac{k_f}{\rho Cp}\left(\frac{\partial^2 T_f}{\partial x^2}+\frac{\partial^2 T_f}{\partial y^2}+\frac{\partial^2 T_f}{\partial z^2}\right) \tag{5}$$

$$k_s\left(\frac{\partial^2 T_s}{\partial x^2}+\frac{\partial^2 T_s}{\partial y^2}+\frac{\partial^2 T_s}{\partial z^2}\right)=0 \tag{6}$$

Where T_f and T_s, k_f and k_s are temperatures and thermal conductivities of fluid and solid materials, respectively.

2.3 Boundary Conditions

The following boundary conditions are specified for the computational domain to close the above mathematical equations, and from the inlet boundary all variables are initiated:

I. At the inlet boundary, "velocity inlet" with temperature and pressure of the nanofluid specified as 30°C (303K) and 1 bar, respectively, while "Pressure outlet" is imposed at the outlet with 0 Pa (gauge pressure).
II. Uniform heat flux condition was applied on the bottom wall by a heating power of 40.5 W from the chip. Thus, Heat flux generated was 45000 W/m^2.
III. The walls experienced no-slip condition (viscous flow) for all directions. Thus velocity gradient exists in fluid and exerts resistance to flow as pressure drop.
IV. No heat loss experienced for all the outside surfaces.

2.4 Thermophysical Properties of the Fluids

The working fluids used in this simulation are aqueous Alumina (Al_2O_3-H_2O), Silica (SiO_2-H_2O) and Copper (Cu-H_2O) nanofluids with volume fractions of 0.005 and 0.008, and thermophysical properties their particles adopted from other study [27], while the base fluid (deionized-water) was extracted from other study [28] at 20℃ and presented in Table 1.

Table 1. Thermophysical properties of water and nanoparticle at Temperature of 303K

Materials	Density (kg/m^3)	Specific heat (J/kgK)	Thermal conductivity (W/mK)	Viscosity (kg/ms)	Particle size (nm)
Water (H_2O)	995.8	4178.4	0.615	798E-06	-
Alumina (Al_2O_3)	3970	765	36	-	<50
Silica (SiO_2)	2220	745	1.38	-	<50
Copper (Cu)	8933	385	401	-	<50

The following relations were used to estimate the thermophysical properties of nanofluids as presented in Eqs. (7) to (10) respectively.

The density of nanofluids was computed using Pak and Cho [29] model:

$$\rho_{nf} = (1-\phi)\rho_{bf} + \phi\rho_p \tag{7}$$

The specific heat of the nanofluids was calculated using Xuan and Roetzel [30] relation:

$$Cp_{nf} = \left[\phi(\rho Cp)_p + (1-\phi)(\rho Cp)_{bf}\right](\rho_{nf})^{-1} \tag{8}$$

The thermal conductivity of the nanofluid (k_{nf}) was calculated using Hamilton and Crosser model [31] which modified Maxwell model for nanofluids to consider Brownian motion and involves shape, distribution and shell structure of particle as well as high concentration; it's given as follows:

$$\frac{k_{nf}}{k_{bf}} = \frac{[k_p+(n-1)k_{bf}-\phi(n-1)(k_{bf}-k_p)]}{k_p+(n-1)k_{bf}+\phi(k_{bf}-k_p)} \tag{9}$$

where empirical shape factor n=3/ψ and for spherical nanoparticles considered in this work, sphericity factor ψ =1.

The viscosity of the nanofluids was calculated using the viscosity correlation proposed by Maiga *et al.,* [32] as follows:

$$\mu_{nf} = \mu_{bf}(1+7.3\phi+123\phi^2) \tag{10}$$

Where, ϕ, Cp, k, and ρ are the concentration of the nanoparticle, heat capacity, thermal conductivity, viscosity, and density respectively. While subscripts bf, p, and nf denote base fluid, nanoparticle and nanofluid respectively.

2.5 Data Reduction

The following Eqs. (11) – (19) were used to estimate the various important thermal and flow parameters of the minichannel heatsink:

The average heat transfer coefficient (h) and Nusselt number (Nu) were respectively obtained by:

$$h = \frac{q}{T_w - T_b} \tag{11}$$

$$Nu = \frac{hD_h}{k} \tag{12}$$

Where D_h is hydraulic diameter which is used to expressed non-circular ducts the same way as a tube for dimensional similarity. Its expressed as:

$$D_h = \frac{4A}{P} = \frac{2(\acute{W} \cdot \dot{H})}{\acute{W} \cdot \dot{H}} \tag{13}$$

While, the area (A) and wetted perimeter (P) were computed from the Eq. (14) and Eq. (15), respectively:

$$A = \frac{1}{2} * (W_t + W_b) * \dot{H} \tag{14}$$

$$P = (W_t + W_b) + 2 * \dot{H} \tag{15}$$

Where: $\dot{H}$, W_t and W_b represent the slant height, widths at the top and bottom sections of the fluid domain.

Using the relation of Reynolds number, the velocity of the base fluid was estimated as follows:

$$Re = \frac{\rho u D_h}{\mu} \tag{16}$$

However, to take into cognizance the impact of base fluid during the nanofluid dispersion, its velocity was estimated from the following expression:

$$u_{nf} = \frac{\rho_{bf}}{\rho_{nf}} \frac{\mu_{nf}}{\mu_{bf}} u_{bf} \tag{17}$$

The frictional resistance of the fluid was obtained from Darcy-Welsbach relation as:

$$f = \frac{2\Delta P}{\rho u^2} \left(\frac{D_h}{L} \right) \tag{18}$$

where q, D_h, L, u, k, T_w, and T_b are the heat flux, hydraulic diameter, channel length, fluid velocity, the thermal conductivity, average temperatures on the wall and bulk fluid, respectively.

The Pressure loss ΔP from Eq. (18) was obtained as an aggregated effect of entrance and exit losses, effects at the developing region and frictional losses:

$$\Delta P = ((P_i - P_o) * \rho \Delta u^2) \tag{19}$$

Where Pi, Po, Δu are the pressure inlet, pressure outlet, and variation of velocity between inlet and outlet, respectively.

The performance of flow in the minichannel was evaluated using pumping power as:

$$PP = \Delta P . \dot{V} \tag{20}$$

3. Numerical Procedure using CFD

A commercial CFD solver, ANSYS FLUENT 17 was used in modeling the three-dimensional forced convection flow and heat transfer. The control volume approach in the Finite Volume Method (FVM) was used in the simulation. The discretization of the convective and diffusive terms was executed with a second-order upwind interpolation scheme, while the velocity and pressure fields were coupled using Semi-Implicit Method for Pressure-Linked Equations (SIMPLE) algorithm introduced by Spalding and Patankar [33]. The convergence criteria set when the normalized residual values for all the variables fell below 10^{-6}.

3.1 Grid Sensitivity Study

Checking of grid independence of the solution was conducted to ensure that the simulation results have no reliance on the size and the number of generated cells. Five different hexahedral mapped mesh generated by edge-sizing along x, y and z coordinates was used for all the simulations with various grids of sizes from 600000 (50x40x300) to 1228800 (64x64x300) and coded M1-M5, respectively. Figure 2 show the meshing of the computational domain used in the analysis.

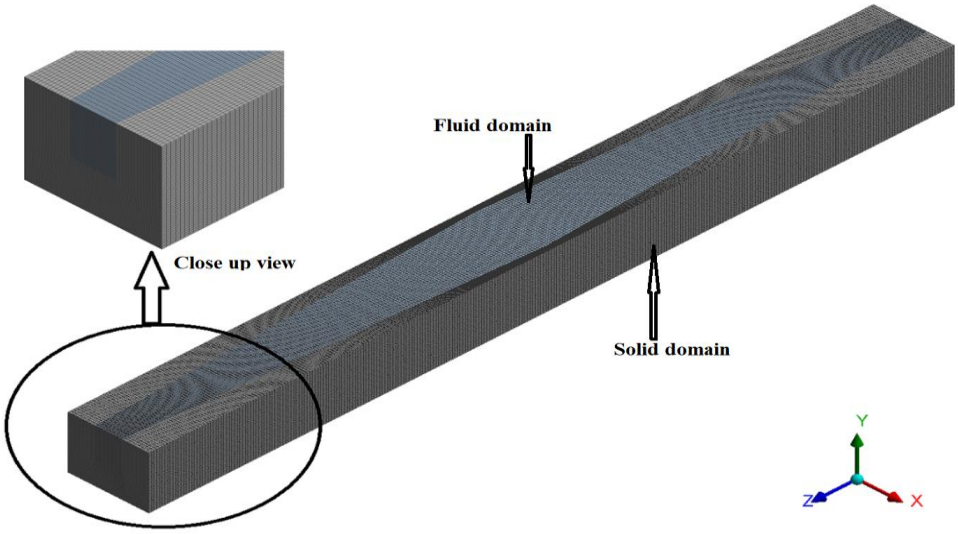

Fig. 2. 3D Mesh of the computational domain

The relative error of the desired parameters was computed using the following equation [34]:

$$e(\%) = \left|\frac{J_2 - J_1}{J_1}\right| \times 100 \quad (18)$$

Where J signifies any parameter; such as Nusselt number, pressure drops, friction factor, and temperature, while J_1 and J_2 signify the parameter values acquired from finest grids and other grids, respectively.

The relative error in the Nusselt numbers between second grid (M2) to the fourth grid (M4) is insignificant, and the solutions on the grids with 900000 and 1228800 elements are found to be below 0.5%. A similar trend was exhibited for friction factor between M2 to M4, while the error is nearly 3% for 600000 grids elements as shown in Figure 3, hence, grid M3 with sizes of 900000 was used for all the simulations in this study to save computing time and memory.

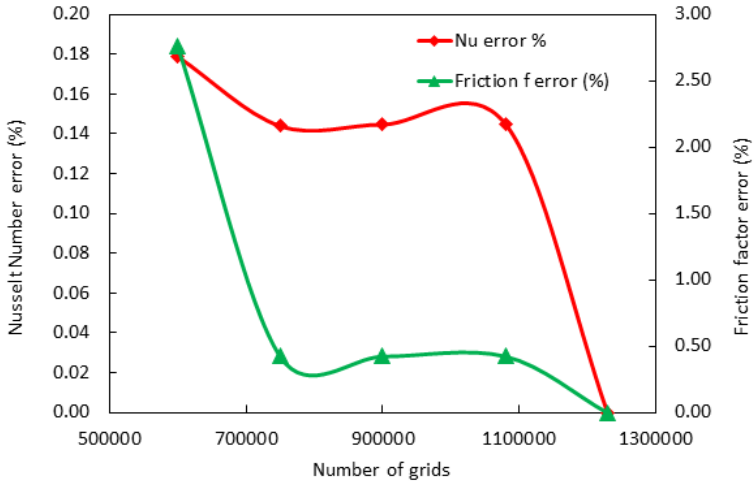

Fig. 3. Relative errors in Nusselt number and Friction factor for grid test

3.2 Validation of Numerical Results

The validation of numerical data to substantiate the ability of the solver to accurately and reliably predict the outcomes achieved through comparison with established correlations in the literature due to non-availability of experimental results in diverging-converging minichannels. Sieder-Tate [35] and Blasius relation [36] for the fully developed laminar region employed for Nusselt number enhancement and frictional resistance; respectively.

Figure 4 illustrated the comparisons of the numerical and established correlations of the average Nusselt number and friction factor using deionized water for the range of Reynolds numbers. The Nusselt number increased as the Reynolds number increases in the DCMCHS. The Sieder-Tate correlation overpredicts the average Nusselt number for the base fluid at Re 2000 and 2300 by about 8% and 6%, respectively as shown in Figure 4(a). For the friction factor, Figure 4(b) indicates the deviation of the numerical friction factor from the theoretical values of Blasius around 4% and 10% lower at 2000 and 2300 Reynolds numbers, respectively because of the increase of pressure drops as the flow velocity increases at the entrance of the channel, and to the assumptions made in the mathematical formulation of the simulation. Thus, the numerical results appreciably well predicted by the method employed since the deviations of the average Nusselt numbers and friction factor from the established correlations used is within ±10%.

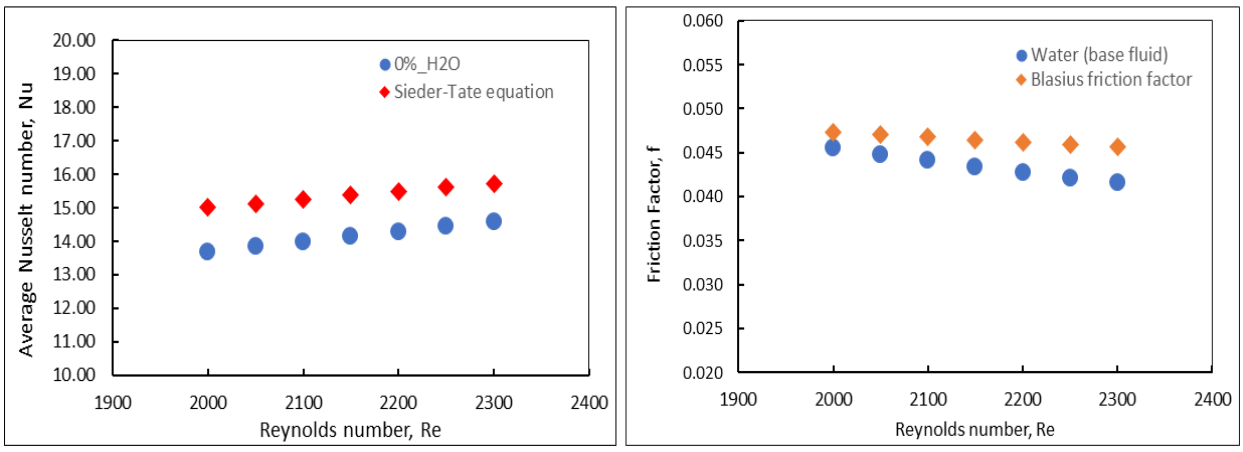

Fig. 4. Validation of results of (a) Nusselt number and (b) friction factor with Reynolds number

4. Results and Discussion

Numerical simulations were conducted using three different nanoparticles made up of Al_2O_3, Cu and SiO_2, with deionized water as the base fluid for concentrations of 0.5 and 0.8 % volume, the range of Reynolds numbers from 2000 to 2300 and heat flux of 45 kW/m^2.

4.1 Effect of Nanofluid Concentration On Heat Transfer Augmentation

The concentration of the nanofluid shows a linear relationship with the average values of Nusselt number as shown in Figure 5(a) and 5(b), respectively. As volume concentration and flow velocity increases, the average Nusselt number also increases. Al_2O_3-H_2O has the highest enhancement in Nusselt number of about 3% at Re of 2300 and a concentration of 0.8 %, its followed by SiO_2-H_2O and Cu-H_2O with 1.9% and 1.3%, respectively. This enhancement in the Nusselt number as nanofluid concentration increase was due to an increase in fluid velocity and mixing of flow. A similar trend exhibited at a concentration of 0.5% but with less enhancement.

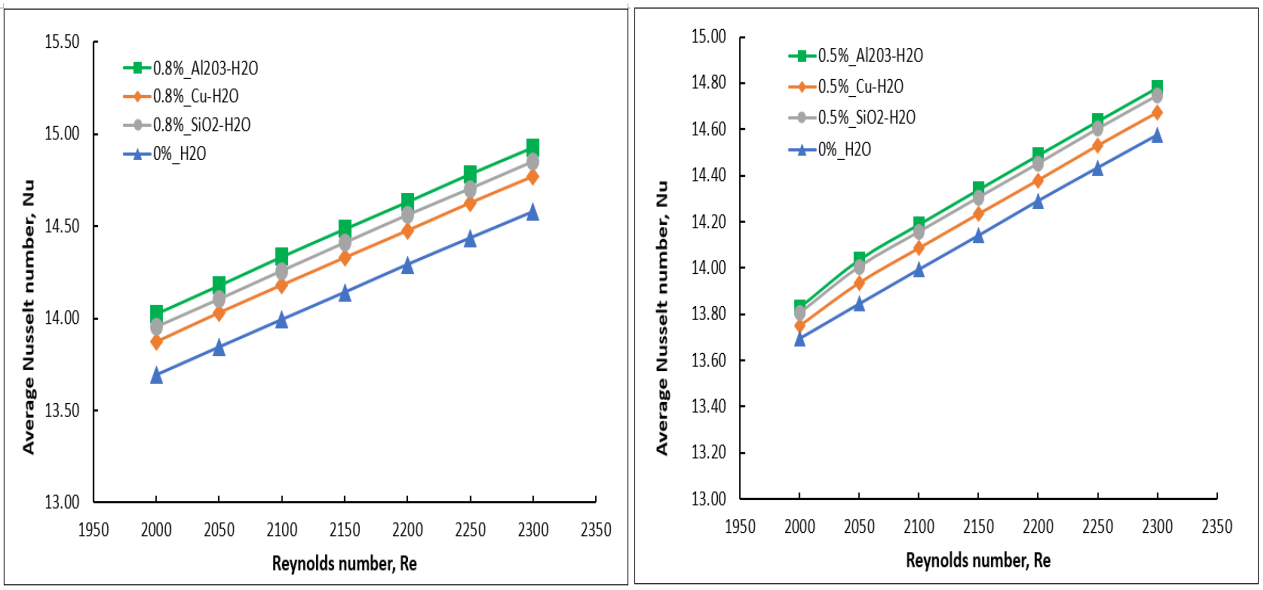

Fig. 5. Effect of nanofluid concentrations on average Nusselt number (a) 0.8% and (b) 0.5%

Similarly, the concentration of the nanofluid and Reynold number plays a significant role in the enhancement of the Heat transfer coefficient as shown in Figure 6(a) and 6(b). As volume concentration and Reynolds number increases, the surface heat transfer coefficient (HTC) also increases with the highest and lowest enhancement for Al_2O_3-H_2O and SiO_2-H_2O respectively. This enhancement is attributed to thermal conductivity, though Cu-H_2O having the highest thermal conductivity value than the other nanofluids should show better enhancement, its density, and increased frictional resistance may affect its HTC enhancement. However, it's evident that all the nanofluid showed remarkable improvement than water at all Reynolds number and concentrations.

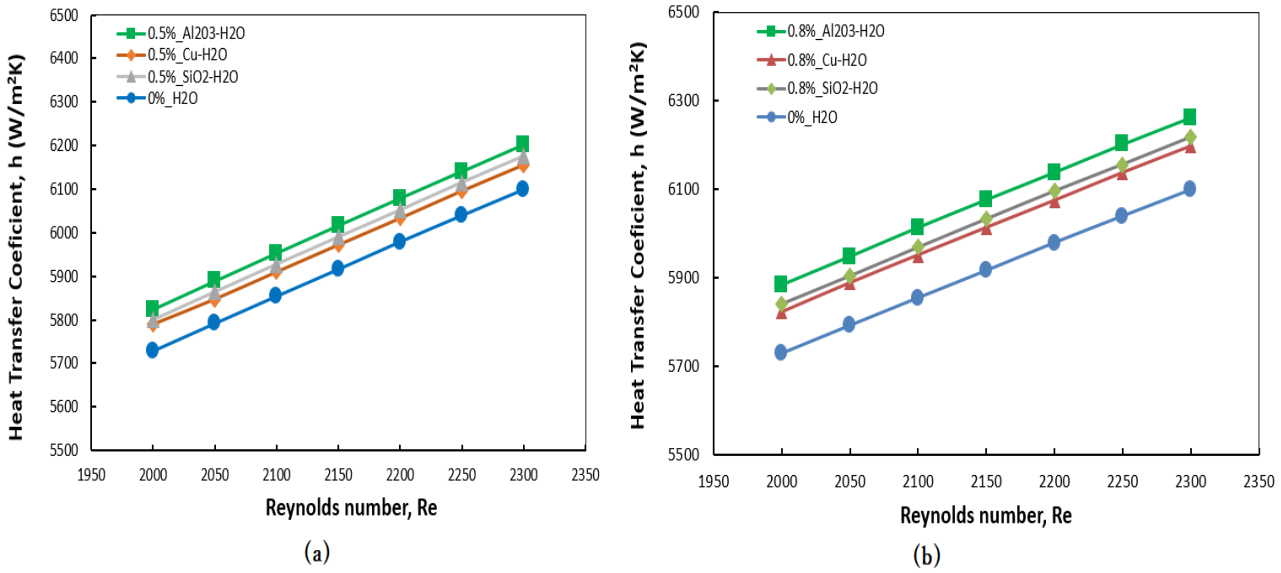

Fig. 6. Effect of nanofluid concentrations on Heat Transfer Coefficient (a) 0.8% and (b) 0.5%

4.2 Effect of Nanofluid Concentration And Types On Pressure Drops

Figure 7 illustrates the variation of pressure drops as a function of Reynolds number. Increase in physical thermal properties of nanofluid over water particularly viscosity leads to the increase in pressure drop from about 7% to about 13 % for the concentrations of 0.5 % and 0.8 %, respectively. SiO_2-H_2O nanofluid has the highest pressure drop due to its low viscosity ratio compared to the other two nanofluids. The increase in pressure drop may be due to increase in velocity as the concentration and viscosity increases as well as expansion and contraction of the flow passage which disturbs the boundary layer and enhances the heat transfer.

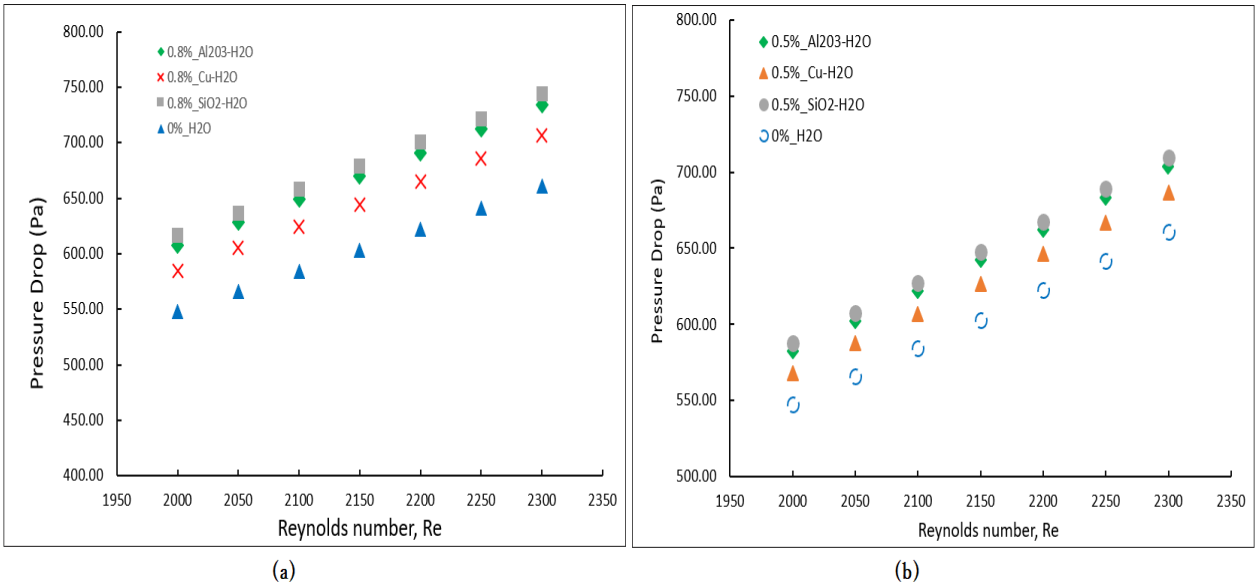

Fig. 7. Variation of Pressure drops with Reynolds number for (a) 0.8% and (b) 0.5%

Figure 8 illustrates the variation of friction factor with Reynolds number for the selected nanofluids at the specified concentrations where all the nanofluids have shown a similar friction factor for all concentrations. The friction factor decreases as the Reynolds number increase. Also, the

variation of the friction coefficient with water is also negligible, hence changes in viscosity of the nanofluids due to the addition of nanoparticles to deionized water has little influence on its friction factor.

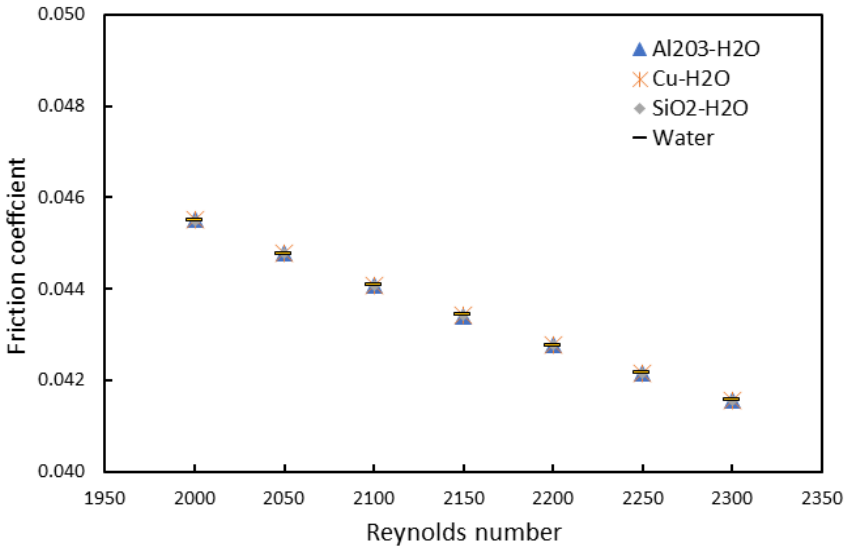

Fig. 8. Friction factor variations with Reynolds number for the water and different nanofluids

During the cooling process, the geometrical nature of the minichannel affects the fluid flow which leads to changes in velocity and consequently affects pressure drop along the passage. However, the system must supplement the flow with additional pumping power to overcome the effect of pressure loss. The pumping power expressed in Eq. (20). Figure 9 Illustrated the effect of different nanofluids on pumping power of the DCMCH against Reynold number. The pumping power increases with an increase in the Reynolds number. Deionized water has the lowest pumping power compared to all the nanofluids. There is an increase in pumping power when the concentrations of nanofluids increases. SiO_2-H_2O has the highest pumping power amongst the nanofluids due to its lowest density since the pumping power has an inverse relationship with density. Another factor that affects pumping power is viscosity since the flow resistance would increase, thus causing pressure loss.

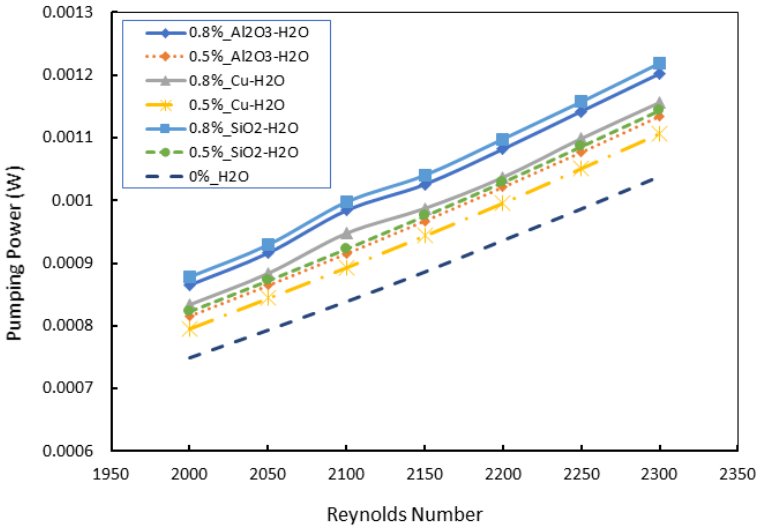

Fig. 9. Effect of nanofluids on pumping power of the DCMCH

4.3 Variation of Temperature with The Flow Of Fluids In The Minichannel

Figure 10 shows the changes in temperature due to the flow of fluids in the DCMCH for the different volume concentrations and flow velocities. The variation of wall temperature decreases with increasing velocity. Since Heat transfer coefficient has an inverse relation with temperature variation from the Newtons law of cooling, Al_2O_3-H_2O nanofluid having highest heat transfer enhancement than other nanofluids indicated the least temperature value on the walls of the minichannel as depicted in Figure 10(a). On the contrary, it showed the highest value of temperature at the outlet which affirms its ability to remove the heat flux from the walls to the core of the minichannel and finally conveys it to the outlet as shown in Figure 10(b). SiO_2-H_2O due to its low thermal conductivity than other nanofluids has the least outlet temperature.

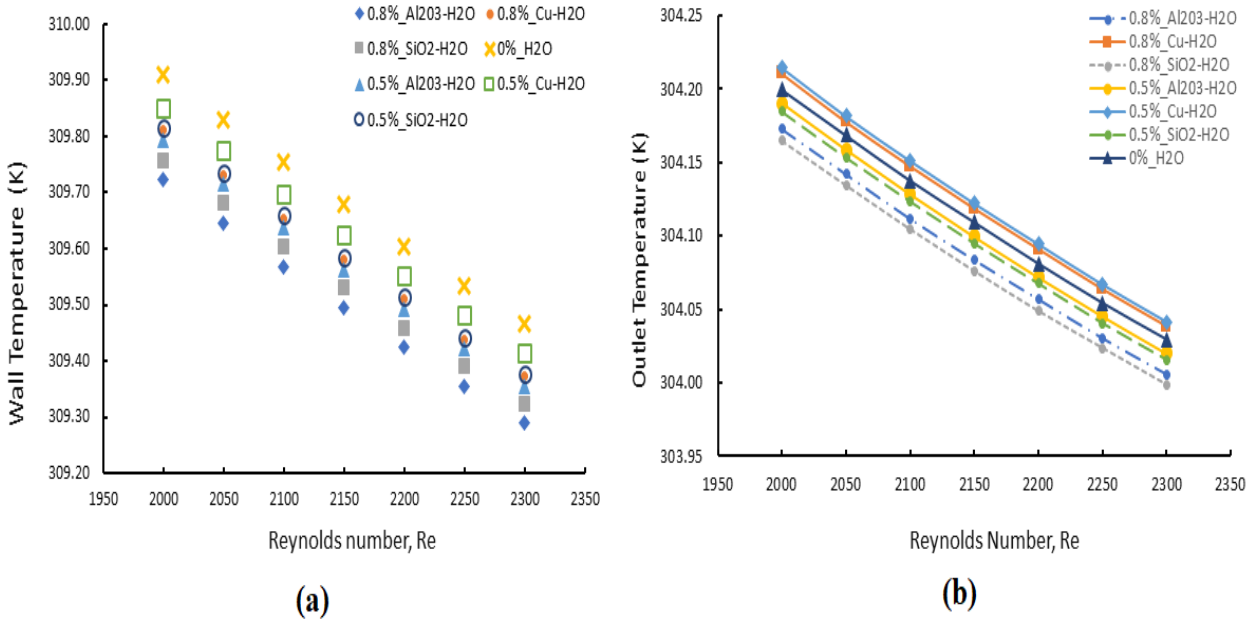

Fig. 10. Variation of wall temperatures on the walls and at the outlet with Reynolds number

Also, water has the highest wall temperature and relatively high outlet temperature than other nanofluids below 0.5% concentration, which confirms its poor potentials in heat transfer enhancement. There is an enhancement of about 28% by the Al_2O_3-H_2O compared to deionized water obtained at Re 2000 and volume fraction of 0.008. The contours of temperature were extracted to observe the physics occurred during the simulations. From Figure 11, the thickness of the boundary layer is significant toward the center and still noticeable up to the minichannel exit since the nanofluids remove the heat flux and convey it to the exit. The thickness of the boundary layer is higher in water due to the absence of nanoparticles that may remove the heat through the Brownian motion effect.

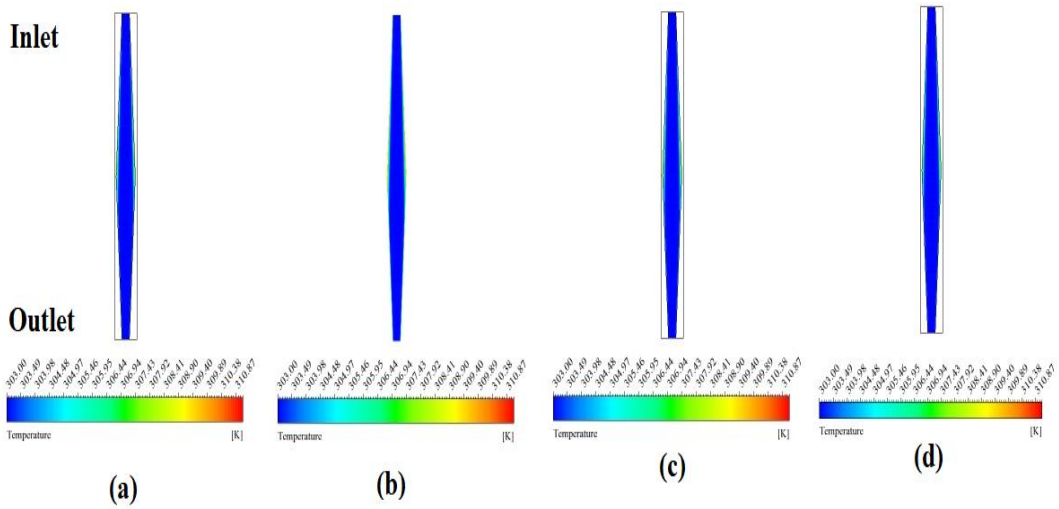

Fig. 11. Contours of Temperature for nanofluids at Re 2300 and concentration of 0.8% vol : (a) Al_2O_3-H_2O, (b) Cu-H_2O, (c) SiO_2-H_2O and (d) H_2O

4.4 Performance Factor

The Combined effect of Nusselt number (*Nu)* and friction factor (*f*) was employed to assess the overall hydrothermal behavior of the nanofluids in the DCMCH using Performance evaluation criterion (PEC) as expressed in Eq. 17 [37]:

$$\eta = \frac{Nu_{nf}/\mathrm{Nu}_{bf}}{\left(f_{nf}/f_{bf}\right)^{1/3}} \tag{17}$$

Where, subscripts nf and bf represent nanofluid and base fluid, respectively.

As highlighted in Figure 12, the performance factor for the nanofluids fell between 1.00 – 1.03, and it increases with increase in concentration and velocity of flow. Since Nusselt number enhancement is higher than friction changes, the performance factor is above unity which indicates the applicability of the geometry in the improvement of heat transfer.

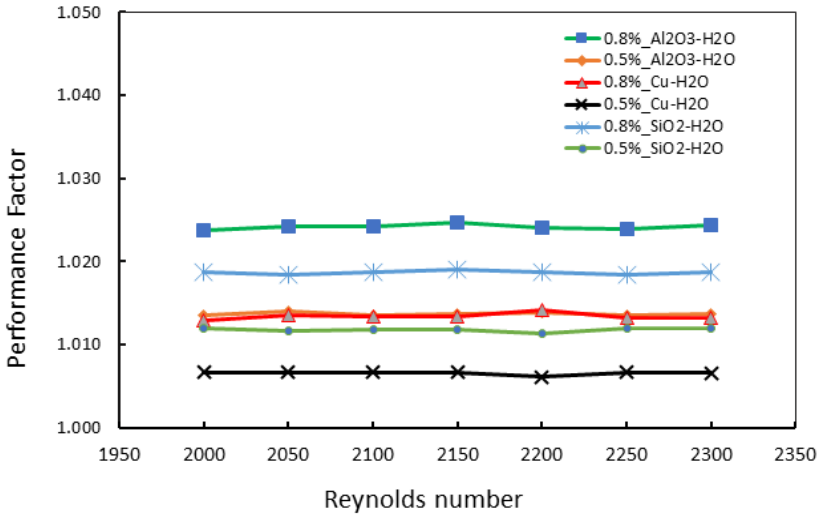

Fig. 12. Performance factors for the nanofluids at 0.5 and 0.8 % concentrations

5. Conclusions

Numerical analysis of heat transfer and fluid flow characteristics of the divergent-convergent minichannel heat sink (DCMCHS) has been studied using three distinct nanofluids, namely Al_2O_3-H_2O, Cu-H_2O, and SiO_2-H_2O. Comparison of results from this study with the established experimental results from the literature, shown a good agreement. The effect of nanofluid was evaluated and observed to influence the heat transfer and flow of fluids in the divergent-convergent minichannel heat sink. The following conclusions were drawn from this investigation:

I. The addition of nanoparticles to the base fluid increased the heat transfer coefficient due to the rising heat flux. Viscosity and density have a significant effect on the flow of the nanofluids.
II. There is a significant influence of Reynolds number on heat transfer enhancement on both the base fluid and the nanofluid. Recirculation and vortices creation enhance flow mixing at the middle of the channel because of deceleration and acceleration of the flow.
III. Friction factor increases slightly due to corrugation of the channel passage due to divergence and convergence nature, and it decreases with increase in Reynolds number. The trend is similar across all the volume fractions.
IV. The enhancement in heat transfer coefficient is higher in Al_2O_3-H_2O followed by SiO_2-H_2O and Cu-H_2O. Higher thermal conductivity of the nanofluid over water and Brownian diffusion played a vital role in this enhancement.
V. Based on the pumping power and the Performance factor, the divergent-convergent minichannel has better potential in terms of provision of adequate cooling of thermal devices with minimal pressure drop and pumping power. which is a factor to indicate the augmentation in heat transfer of nanofluid over base fluid was found to be 1.01
VI. Significant improvement in heat transfer and the hydrodynamic impact could be achieved and better predicted if the numerical analysis extended to the turbulent regime and moderately higher volume concentration.

Acknowledgment

This research was funded by a grant from Takasago Thermal and Environmental System, MJIIT, UTM Kuala Lumpur. Malaysia (Grant R. K130000.7343.4B314).

References

[1] Albojamal, Ahmed, and Kambiz Vafai. "Analysis of single phase, discrete and mixture models, in predicting nanofluid transport." *International Journal of Heat and Mass Transfer* 114 (2017): 225-237.
[2] Kakaç, Sadık, and Anchasa Pramuanjaroenkij. "Single-phase and two-phase treatments of convective heat transfer enhancement with nanofluids–A state-of-the-art review." *International journal of thermal sciences* 100 (2016): 75-97.
[3] Kumar, Vivek, and Jahar Sarkar. "Two-phase numerical simulation of hybrid nanofluid heat transfer in minichannel heat sink and experimental validation." *International Communications in Heat and Mass Transfer* 91 (2018): 239-247.
[4] Ma, Lei, Xuxin Zhao, Hongyuan Sun, Qixing Wu, and Wei Liu. "Experimental study of single phase flow in a closed-loop cooling system with integrated mini-channel heat sink." *Entropy* 18, no. 6 (2016): 128.
[5] Moraveji, Mostafa Keshavarz, and Reza Mohammadi Ardehali. "CFD modeling (comparing single and two-phase approaches) on thermal performance of Al2O3/water nanofluid in mini-channel heat sink." *International Communications in Heat and Mass Transfer* 44 (2013): 157-164.
[6] Saeed, Muhammad, and Man-Hoe Kim. "Heat transfer enhancement using nanofluids (Al2O3-H2O) in mini-channel heatsinks." *International Journal of Heat and Mass Transfer* 120 (2018): 671-682.

[7] Choi, Stephen US, and Jeffrey A. Eastman. *Enhancing thermal conductivity of fluids with nanoparticles*. No. ANL/MSD/CP-84938; CONF-951135-29. Argonne National Lab., IL (United States), 1995.
[8] Ilyas, Suhaib Umer, Rajashekhar Pendyala, Marneni Narahari, and Lim Susin. "Stability, rheology and thermal analysis of functionalized alumina-thermal oil-based nanofluids for advanced cooling systems." *Energy conversion and management* 142 (2017): 215-229.
[9] Khaleduzzaman, S.S., et al. *Stability of Al2O3-water nanofluid for electronics cooling system*. in *6th BSME International Conference on Thermal Engineering (ICTE 2014)*. 2015. Elsevier Ltd.
[10] Bahiraei, Mehdi, and Saeed Heshmatian. "Application of a novel biological nanofluid in a liquid block heat sink for cooling of an electronic processor: thermal performance and irreversibility considerations." *Energy Conversion and Management* 149 (2017): 155-167.
[11] Arshad, Waqas, and Hafiz Muhammad Ali. "Experimental investigation of heat transfer and pressure drop in a straight minichannel heat sink using TiO2 nanofluid." *International Journal of Heat and Mass Transfer* 110 (2017): 248-256.
[12] Huminic, Gabriela, Angel Huminic, Claudiu Fleaca, Florian Dumitrache, and Ion Morjan. "Thermo-physical properties of water based SiC nanofluids for heat transfer applications." *International Communications in Heat and Mass Transfer* 84 (2017): 94-101.
[13] Diao, Y. H., C. Z. Li, J. Zhang, Y. H. Zhao, and Y. M. Kang. "Experimental investigation of MWCNT–water nanofluids flow and convective heat transfer characteristics in multiport minichannels with smooth/micro-fin surface." *Powder Technology* 305 (2017): 206-216.
[14] Hussien, Ahmed A., Mohd Z. Abdullah, Nadiahnor Md Yusop, Al-Nimr Moh'd A, Muataz A. Atieh, and Mohammad Mehrali. "Experiment on forced convective heat transfer enhancement using MWCNTs/GNPs hybrid nanofluid and mini-tube." *International Journal of Heat and Mass Transfer* 115 (2017): 1121-1131.
[15] Afzal, Asif, A. D. Samee, R. K. Razak, and M. K. Ramis. "Heat transfer characteristics of MWCNT nanofluid in rectangular mini channels." *International Journal Of Heat And Technology* 36, no. 1 (2018): 222-228.
[16] Muhammad, Nura Mu'az, and Nor Azwadi Che Sidik. "Applications of Nanofluids and Various Minichannel Configurations for Heat Transfer Improvement: A Review of Numerical Study." *Journal of Advanced Research in Fluid Mechanics and Thermal Sciences* 46, no. 1 (2018): 49-61.
[17] Elsheikh, A. H., S. W. Sharshir, Mohamed E. Mostafa, F. A. Essa, and Mohamed Kamal Ahmed Ali. "Applications of nanofluids in solar energy: a review of recent advances." *Renewable and Sustainable Energy Reviews* 82 (2018): 3483-3502.
[18] Ahmed, Hamdi E., B. H. Salman, A. Sh Kherbeet, and M. I. Ahmed. "Optimization of thermal design of heat sinks: A review." *International Journal of Heat and Mass Transfer* 118 (2018): 129-153.
[19] Mahian, Omid, Ali Kianifar, Ahmet Z. Sahin, and Somchai Wongwises. "Performance analysis of a minichannel-based solar collector using different nanofluids." *Energy conversion and management* 88 (2014): 129-138.
[20] Sohel, M. R., Saidur Rahman, Mohd Sabri, Mohd Faizul, M. M. Elias, and S. S. Khaleduzzaman. "Investigation of Heat Transfer Performances of Nanofluids Flow through a Circular Minichannel Heat Sink for Cooling of Electronics." In *Advanced Materials Research* 832 (2014): 166-171.
[21] Ismail, Mohammed, Shahram Fotowat, and Amir Fartaj. *Transient Response of Minichannel Heat Exchanger Using Al 2 O 3-EG/W Nanofluid*. No. 2016-01-0229. SAE Technical Paper, 2016.
[22] Hussien, Ahmed A., Mohd Z. Abdullah, and Al-Nimr Moh'd A. "Single-phase heat transfer enhancement in micro/minichannels using nanofluids: theory and applications." *Applied energy* 164 (2016): 733-755.
[23] Khoshvaght-Aliabadi, M., Z. Arani, and F. Rahimpour. "Influence of Al2O3–H2O nanofluid on performance of twisted minichannels." *Advanced Powder Technology* 27, no. 4 (2016): 1514-1525.
[24] Raheem Kadhim Ajeel, Wan Saiful-Islam Wan Salim, and Khalid Hasnan."Heat Transfer Enhancement in Semicircle Corrugated Channel: Effect of Geometrical Parameters and Nanofluid." *Journal of Advanced Research in Fluid Mechanics and Thermal Sciences* 53, no. 1 (2019): 82-94.
[25] Hasan, Husam Abdulrasool, Zainab Alquziweeni, and Kamaruzzaman Sopian. "Heat Transfer Enhancement Using Nanofluids For Cooling A Central Processing Unit (CPU) System." *Journal of Advanced Research in Fluid Mechanics and Thermal Sciences* 51, no. 2 (2018): 145-157.
[26] Muhammad, N. M., and N. A. C. Sidik. "Numerical analysis on thermal and hydraulic performance of diverging-converging minichannel heat sink using Al2O3-H2O nanofluid." In *IOP Conference Series: Materials Science and Engineering*, vol. 469, no. 1, p. 012046. IOP Publishing, 2019.
[27] Abdelrazek, Ali H., Omer A. Alawi, S. N. Kazi, Nukman Yusoff, Zaira Chowdhury, and Ahmed AD Sarhan. "A new approach to evaluate the impact of thermophysical properties of nanofluids on heat transfer and pressure drop." *International Communications in Heat and Mass Transfer* 95 (2018): 161-170.
[28] Yunus, C.A. and J.G. Afshin, *Heat and mass transfer: fundamentals and applications*. 2011, New Delhi, India: Tata McGraw-Hill.

[29] Pak, Bock Choon, and Young I. Cho. "Hydrodynamic and heat transfer study of dispersed fluids with submicron metallic oxide particles." *Experimental Heat Transfer an International Journal* 11, no. 2 (1998): 151-170.
[30] Xuan, Yimin, and Wilfried Roetzel. "Conceptions for heat transfer correlation of nanofluids." *International Journal of heat and Mass transfer* 43, no. 19 (2000): 3701-3707.
[31] Hamilton, R. L㎡, and O. K. Crosser. "Thermal conductivity of heterogeneous two-component systems." *Industrial & Engineering chemistry fundamentals* 1, no. 3 (1962): 187-191.
[32] Maiga, Sidi El Becaye, Samy Joseph Palm, Cong Tam Nguyen, Gilles Roy, and Nicolas Galanis. "Heat transfer enhancement by using nanofluids in forced convection flows." *International journal of heat and fluid flow* 26, no. 4 (2005): 530-546.
[33] Anderson, D., J.C. Tannehill, and R.H. Pletcher, *Computational fluid mechanics and heat transfer*. 2016: CRC Press.
[34] Ghani, Ihsan Ali, Natrah Kamaruzaman, and Nor Azwadi Che Sidik. "Heat transfer augmentation in a microchannel heat sink with sinusoidal cavities and rectangular ribs." *International Journal of Heat and Mass Transfer* 108 (2017): 1969-1981.
[35] Liu, Dong, and Leyuan Yu. "Single-phase thermal transport of nanofluids in a minichannel." *Journal of Heat Transfer* 133, no. 3 (2011): 031009.
[36] Abdolbaqi, M. Kh, Rizalman Mamat, Nor Azwadi Che Sidik, W. H. Azmi, and P. Selvakumar. "Experimental investigation and development of new correlations for heat transfer enhancement and friction factor of BioGlycol/water based TiO2 nanofluids in flat tubes." *International Journal of Heat and Mass Transfer* 108 (2017): 1026-1035.
[37] Xia, G. D., R. Liu, J. Wang, and M. Du. "The characteristics of convective heat transfer in microchannel heat sinks using Al2O3 and TiO2 nanofluids." *International Communications in Heat and Mass Transfer* 76 (2016): 256-264.